Effect of asymmetry in a binary state on the collective behavior of a system with spatially modulated interaction and quenched randomness

Kosuke Hamaguchi*
Amari Research Unit, Brain Science Institute, RIKEN, 2-1 Hirosawa Wako, Saitama, Japan

Hiromitsu Urano
Department of Complexity Science and Engineering, University of Tokyo, Kashiwanoha 5-1-5, Kashiwa, Chiba, 277-8561, Japan

Masato Okada
Department of Complexity Science and Engineering, University of Tokyo, Kashiwanoha 5-1-5, Kashiwa, Chiba, 277-8561, Japan
and Brain Science Institute, RIKEN, 2-1 Hirosawa Wako, Saitama, Japan

(Received 20 August 2008; revised manuscript received 1 October 2008; published 24 November 2008)

The properties of solid states, biophysical materials, neuronal circuits, and equilibrium states of a many-body system can be studied by using techniques in statistical physics. It has been common practice to represent a system composed of binary state units by using an Ising spin network where each unit has symmetric $\{-1,1\}$ states. However, the asymmetry or symmetry of the binary states of the units can affect the property and ergodicity of the system, but better understanding of the quantitative difference is still needed. We compare systems of binary units with symmetric or asymmetric states. The network has spatially modulated interaction with quenched randomness. We can bridge the Ising spin network and McCulloch-Pitts neuron network and analyze the stability of the system via replica method by introducing an interpolating parameter. The effects of the asymmetry states affect the multistability of the system and the stability of replica-symmetry solutions.

DOI: 10.1103/PhysRevE.78.051124 PACS number(s): 05.20.−y, 75.10.Nr, 87.85.dq

I. INTRODUCTION

The range of applications for statistical physics has expanded and now covers the fields of information science, communication theory, learning theory, and neuroscience [1]. In studies on the properties of many-body systems composed of binary-state units, it has become common practice to represent the binary state as ± 1 of the spin, and to analyze the system as an Ising spin system. The memory capacity and basin of attraction of associative neural networks have been studied as Ising spins systems [2–4]. On the other hand, in the field of neural networks, a neuron with a binary state of $\{0, 1\}$ is called McCulloch-Pitts neuron and has an asymmetric state. Both Ising spins and McCulloch-Pitts neurons are binary-state units, therefore a transformation of variables exists so that two models become equivalent if the connectivity is homogeneous. However, when a network has quenched randomness as is seen in the Sherrington-Kirkpatrick (SK) model, or in the associative memory models, equivalent transformation of the variables exists unless the external fields of each unit are heterogeneous. Therefore, the effect of quenched randomness can have a different effect on the macroscopic properties of a system, depending on the symmetry of the states of the units.

For example, sparsely encoded associative memory learned with the covariance rule has maximum storage capacity when the Hamiltonian is described by asymmetric states [5]. The covariance rule has bias term a which controls the sparseness of the population activity or population firing rate. The maximum storage capacity is obtained when Ising state S_i is transformed into $S_i - a$ in the Hamiltonian, therefore this transformation introduces asymmetry into Ising spin interactions. Those sparsely encoded associative networks that are tuned to maximize the storage capacity have diverging memory capacity as the population firing rate per memory pattern approaches zero [6,7]. In contrast, an equivalent network with Ising spins with symmetric interaction has a finite memory capacity [8].

In the visual cortex of mammals, many of the neurons in the primary visual cortex have direction and orientation selectivity [9], and in certain species, neurons with similar selectivity cluster and form a column like structure [10]. Furthermore, in the prefrontal cortex of monkeys, there are neurons that are active during the spatial memory task. Depending on the direction of the visual queue position, they maintain their activity even after the external stimulus is off. One possible mechanism to explain such activities is the Mexican-hat-type network where the recurrent interaction forms nearby excitation and distal inhibition [11]. This type of recurrent interaction facilitates the bump activity (locally activated region), and the stability of the bump activity has been studied in several neuron models ranging from analog neurons [12–15] to spiking neurons [16,17].

Most of the Mexican-hat-type networks have neutrally stable states due to the homogeneous assumption of the connectivity rule or neuron properties throughout the population. Due to this neutral stability, the spatial position of the bump states can be easily displaced by several types of noises [16]. When there is moderate heterogeneity in each neuron property, the position of the bump tends to drift, resulting in the loss of spatial working memory [18]. However, the Mexican-hat-type networks with quenched randomness in the Ising

*hamaguchi@neuro.duke.edu;
http://www.brain.riken.jp/labs/mns/hammer/

spin network [19] have shown that large quenched randomness is actually advantageous because it helps to maintain the position of the spatial working memory by having an infinitely large number of local minimums in the energy landscape [19]. However, it is still not fully understood how the results from the Ising spin networks can be translated into the McCulloch-Pitts model networks.

In this paper we used a network with the Mexican-hat interaction with quenched randomness as the model to study the effect of symmetry and/or asymmetry of the binary states of the units on the macroscopic states of the network. We bridged the Ising spin and the McCulloch-Pitts network by introducing an interpolating parameter. We analyzed this system via a replica trick. In Sec. II, the details of the model are given. In Sec. III, the replica-symmetry (RS) ansatz are calculated. In Sec. IV, the replica-symmetry breaking (RSB) conditions are shown. In Sec. V, we show the numerical solutions of the RS solutions with the support of Monte Carlo simulations. Phase diagrams for both the Ising spin and McCulloch-Pitts networks are also presented. In Sec. VI, we conclude and give a discussion.

II. MODEL

We studied the macroscopic properties of a system composed of many binary units interacting with symmetric, spatially organized interactions with quenched randomness. We assumed that each unit can be indexed based on its preference to the external stimuli that is parametrized by a single parameter θ. The parameter θ represents the direction or orientation of the gratings of the visual stimuli [10], or direction of the motion to be stored in a short term spatial working memory [20]. For simplicity, we set $\theta \in [-\pi, \pi)$.

We also assumed that the interaction between units is spatially organized in this parameter space so that the connectivities had effectively Mexican-hat-type interaction. The boundary of parameter space θ is connected by using a periodic boundary condition. The symmetric interaction between the jth and ith units, $J_{\theta_i\theta_j}(=J_{\theta_j\theta_i})$, is given as follows:

$$J_{\theta_i\theta_j} = \frac{J_0}{N} + \frac{J_1}{N}\cos(\theta_i - \theta_j) + \frac{\Delta}{\sqrt{N}} z_{\theta_i\theta_j}, \tag{1}$$

$$z_{\theta_i\theta_j} \sim N(0,1). \tag{2}$$

Here, J_0 is the uniform ferromagnetic interaction, or spatially uniform term, J_1 is the Mexican-hat-type interaction, or spatially modulated term, and $z_{\theta_i\theta_j}=z_{\theta_j\theta_i}$ is a quenched noisy interaction term derived from the Gaussian distribution with mean 0, variance 1. A schematic picture of the network in parameter space θ is shown in Fig. 1.

The position of the ith unit in the parameter space is θ_i, and we describe the binary state of the ith unit as S_{θ_i}. The update rule of the model is

$$\mathrm{Prob}[S_{\theta_i} = \pm 1] = \frac{1 \pm \tanh(\beta h_i)}{2}, \tag{3}$$

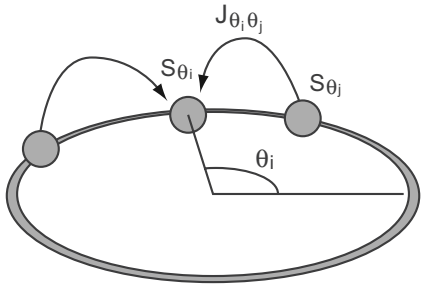

FIG. 1. Network model: N units indexed with $\theta_i \in [-\pi, \pi)$ on a ring are interacting with symmetric $J_{\theta_i\theta_j}$ interactions.

$$h_i = \sum_{\theta_j \neq \theta_i} J_{\theta_i\theta_j}(S_{\theta_j} - b) + h, \tag{4}$$

where h is the external field, and β is the inverse temperature. The Hamiltonian of the system we will study here is

$$H_b(\boldsymbol{S}) = -\frac{1}{2}\sum_{\theta_i,\theta_j} J_{\theta_i\theta_j}(S_{\theta_i} - b)(S_{\theta_j} - b) - h\sum_i (S_{\theta_i} - b) \quad (S_{\theta_i} = \pm 1), \tag{5}$$

where $\boldsymbol{S}$ is the state of the N units, $\boldsymbol{S}=(S_{\theta_1}, S_{\theta_2}, \ldots, S_{\theta_N})$. To compare the Ising spin and the McCulloch-Pitts neuron networks, we have introduced a parameter b to interpolate the two models. When $b=0$, $H_0(\boldsymbol{S})$ is equivalent to the Hamiltonian of the conventional Ising spin networks because the state of a unit is symmetric, $(S_{\theta_i} - b) \in \{-1, 1\}$. On the other hand, when $b=-1$, the effective output is asymmetric, $(S_{\theta_i} - b) \in \{0, 2\}$; this model is intrinsically equivalent to the McCulloch-Pitts-type neuron models in which output takes on the binary values of {0, 1}.

We note that, when $\Delta=0$ (no quenched randomness in the interaction), the Hamiltonian in Eq. (5) is rewritten as

$$H_b(\boldsymbol{S}) = -\frac{1}{2}\frac{J_0}{N}\sum_{\theta_i,\theta_j} S_{\theta_i}S_{\theta_j} - \frac{1}{2}\frac{J_1}{N}\sum_{\theta_i,\theta_j} S_{\theta_i}S_{\theta_j}\cos(\theta_i - \theta_j) + (J_0 b - h)\sum_{\theta_i} S_{\theta_i} + Nb\left(h - \frac{J_0 b}{2}\right). \tag{6}$$

The last constant term does not play any role in determining the equilibrium state. The coefficient of the third term $(J_0 b - h)$ indicates that, the Ising and McCulloch-Pitts networks become equivalent when $h=J_0 b$ because the Hamiltonian does not depend on b. This equivalence does not hold for $\Delta \neq 0$, and the purpose of this work is to understand how the properties of a system change depending on parameter b, and more specifically, to compare Ising spin networks $(b=0)$ and McCulloch-Pitts networks $(b=-1)$.

III. REPLICA CALCULATION OF THE FREE ENERGY AND ORDER PARAMETERS

In this section, we calculate the free energy per neuron and relevant order parameters by using the replica method. To calculate the partition function Z, let us circumvent averaging $\ln Z$ by using

$$\ln Z = \lim_{n\to 0} \frac{Z^n - 1}{n}, \tag{7}$$

which allows us to compute $\ln Z$ from Z^n as a partition function of n copies, replicas, of the original system, writing

$$Z^n = \mathrm{Tr}_{S^1}\mathrm{Tr}_{S^2}\cdots\mathrm{Tr}_{S^n}\exp\left(-\beta\sum_{\alpha=1}^{n} H(S^\alpha)\right) = \mathrm{Tr}_S \exp\left(-\beta\sum_{\alpha=1}^{n} H(S^\alpha)\right), \tag{8}$$

where α is the replica index running from 1 to n. The free energy $F=-\beta^{-1}\ln Z$ is a function of the quenched connection noise $\{z_{\theta_i\theta_j}\}$. We obtain the actual value of F by averaging F with the probability distribution of $z_{\theta_i\theta_j}$. We refer to this average as the configurational average and write $\langle\langle\cdots\rangle\rangle$. The configurational average of free energy is

$$\langle\langle Z^n\rangle\rangle = \mathrm{Tr}_S \int \prod_{\alpha<\beta} dq_0^{\alpha\beta} \prod_\alpha dm_0^\alpha \prod_\alpha dm_c^\alpha \prod_\alpha dm_s^\alpha \exp\left[-\frac{N\beta^2\Delta^2}{2}\sum_{\alpha<\beta}(q_0^{\alpha\beta})^2 - \left(\frac{N\beta J_0}{2} + Nb^2\beta^2\Delta^2\right)\sum_\alpha (m_0^\alpha)^2 - \frac{N\beta J_1}{2}\sum_\alpha [(m_c^\alpha)^2 + (m_s^\alpha)^2] + \frac{(1-b^2)^2\beta^2\Delta^2(N-n)n}{4} + L\right], \tag{9}$$

where

$$L = \sum_{\theta_i}\left[\Delta^2\beta^2\sum_{\alpha<\beta}(S_{\theta_i}^\alpha - b)(S_{\theta_i}^\beta - b)q_0^{\alpha\beta} + (\beta J_0 + 2b^2\beta^2\Delta^2)\sum_\alpha (S_{\theta_i}^\alpha - b)m_0^\alpha + \beta J_1\sum_\alpha (m_c^\alpha\cos\theta_i + m_s^\alpha\sin\theta_i)(S_{\theta_i}^\alpha - b) + [\beta h + b\beta J_0 - \beta^2\Delta^2 b(1-b^2)]\sum_\alpha (S_{\theta_i}^\alpha - b)\right]. \tag{10}$$

Here we define the following order parameters:

$$m_0^\alpha = N^{-1}\sum_i S_{\theta_i}^\alpha - b, \quad q_0^{\alpha\beta} = N^{-1}\sum_i (S_{\theta_i}^\alpha - b)(S_{\theta_i}^\beta - b),$$

$$m_c^\alpha = N^{-1}\sum_i \cos(\theta_i)S_{\theta_i}^\alpha, \quad m_s^\alpha = N^{-1}\sum_i \sin(\theta_i)S_{\theta_i}^\alpha, \tag{11}$$

where m_0 is the magnetization or mean firing rate, q_0 is the spin-glass order parameter, m_c and m_s are the order parameters that show how the spins are aligned in the same direction locally around $\theta=0,\pi/2$. The state of the network is said to be a bump state, or locally activated, if m_c or m_s are nonzero. We must note that m_c and m_s depend on the position of the bump, but our interests are focused on the size and the position of the bump. So we introduce the following transformation to separate the size and position of the bump:

$$(m_1^\alpha)^2 = (m_c^\alpha)^2 + (m_s^\alpha)^2, \tag{12}$$

$$\phi^\alpha = \tan^{-1}(m_s^\alpha/m_c^\alpha). \tag{13}$$

Replica-symmetry ansatz. We assume the replica symmetry, which is $q_0^{\alpha\beta}=q_0$, $m_0^\alpha=m_0$, $m_1^\alpha=m_1$, $\phi^\alpha=\phi$ and derive the saddle-point equations for the replica-symmetric solution. To arrive at an effective single-site problem, the Gaussian integral $\exp[\frac{a}{2}(S_{\theta_i}-b)^2]=\int Dz_{\theta_i}\exp[\sqrt{a}(S_{\theta_i}-b)z_{\theta_i}]$, where $\int Dz_{\theta_i} = (2\pi)^{-1/2}\int_{-\infty}^{\infty}\exp(-z_{\theta_i}^2/2)$ is operated to $\mathrm{Tr}_S e^L$,

$$\mathrm{Tr}_S e^L = \mathrm{Tr}_S\prod_{\theta_i}\int Dz_{\theta_i}\exp\left[\left(\beta\Delta\sqrt{q_0}z_{\theta_i} - \frac{\beta^2\Delta^2}{2}nq_0 + \beta J_0 m_0 + \beta J_1 m_1\cos(\theta_i+\phi) + \beta h + C\right)\sum_\alpha (S_{\theta_i}^\alpha - b)\right] = \prod_{\theta_i}\int Dz_\theta\{\exp[(1-b)\Psi_{\theta_i}] + \exp[(-1-b)\Psi_{\theta_i}]\}^n \exp\left(-\frac{Nn\beta^2\Delta^2}{2}q_0\right), \tag{14}$$

and

$$\Psi_{\theta_i} = \beta\Delta\sqrt{q_0}z_{\theta_i} + \beta J_0 m_0 + \beta J_1 m_1\cos(\theta_i+\phi) + \beta h + C, \tag{15}$$

$$C = b\beta^2\Delta^2(2bm_0 + q_0 + b^2 - 1). \tag{16}$$

The replica-symmetry assumption simplifies Eq. (9) to

$$\langle\langle Z^n\rangle\rangle = \int dq_0 dm_o dm_c dm_s \exp\left(-\frac{Nn(n-1)\Delta^2\beta^2}{4}q_0^2 - \frac{Nn\beta J_0 + 2b^2\beta^2\Delta^2}{2}m_0^2 - \frac{Nn\beta J_1}{2}m_1^2 + \frac{(1-b^2)^2\beta^2\Delta^2(N-n)n}{4}\right)$$
$$\times\exp\left[\sum_{\theta_i}\ln\left(\int Dz_\theta\{\exp[(1-b)\Psi_{\theta_i}] + \exp[(-1-b)\Psi_{\theta_i}]\}^n\right)\right]. \tag{17}$$

The free energy per neuron, $\beta[f] = -\frac{1}{N}[\ln Z] = -\lim_{n\to 0}\frac{[Z^n]-1}{Nn}$ is evaluated in the thermodynamical limit. The summation of θ_i is now replaced by an integral with θ. The free energy per neuron is

$$-\beta[f] = \frac{\beta^2\Delta^2}{4}(1-b-q_0)^2 - \frac{\beta J_0 + 2b^2\beta^2\Delta^2}{2}m_0^2$$
$$-\frac{\beta J_1}{2}m_1^2 + \frac{1}{2\pi}\int_{-\pi}^{\pi}d\theta\int_{-\infty}^{\infty}Dz\ln\{\exp[(1-b)\Psi_\theta]$$
$$+\exp[(-1-b)\Psi_\theta]\}. \tag{18}$$

The order parameters m_0, m_1, ϕ, and q_0 are determined through the following saddle-point equations:

$$m_0 = \int\frac{d\theta}{2\pi}\int Dz(\tanh\Psi_\theta - b), \tag{19}$$

$$m_1 = \int\frac{d\theta}{2\pi}\int Dz\cos(\theta-\phi)(\tanh\Psi_\theta - b), \tag{20}$$

$$0 = \int\frac{d\theta}{2\pi}\int Dz\sin(\theta-\phi)(\tanh\Psi_\theta - b), \tag{21}$$

$$q_0 = \int\frac{d\theta}{2\pi}\int Dz(\tanh\Psi_\theta - b)^2. \tag{22}$$

IV. CALCULATION OF RSB CONDITIONS

The saddle-point equations in Eqs. (19)–(22) give the equilibrium points (local minimum, maximum, and saddles) in the free-energy landscape under the replica-symmetry (RS) assumption. The stability of the RS solutions is given by the eigenvalue of the Hessian matrix around a RS solution [21]. The instability condition of RS solutions is called replica-symmetry breaking (RSB) condition. To calculate the RSB condition, we expand the free energy around a RS solution up to the second order. We first rewrite the $\langle\langle Z^n\rangle\rangle$ before $n\to 0$ as

$$\langle\langle Z^n\rangle\rangle \approx 1 + Nn\left(-\frac{\beta^2\Delta^2}{2n}\sum_{\alpha<\beta}(q_0^{\alpha\beta})^2 - \frac{\beta J_0 + 2b^2\beta^2\Delta^2}{2n}\sum_\alpha(m_0^\alpha)^2 - \frac{\beta J_1}{2n}\sum_\alpha(m_1^\alpha)^2 + \frac{1}{Nn}\ln\mathrm{Tr}_S e^L + \frac{(1-b^2)^2\beta^2\Delta^2}{4}\right). \tag{23}$$

By using the following transformation, $y^{\alpha\beta}\equiv\Delta' q_0^{\alpha\beta}$, $x^\alpha\equiv\sqrt{K_0}m_0^\alpha$, $z^\alpha\equiv\sqrt{K_1}m_1^\alpha$, where $\Delta' = \beta\Delta$, $K_0 = (\beta J_0 + 2b^2\beta^2\Delta^2)$, and $K_1 = \beta J_1$, the free energy per neuron can be written as

$$-\beta\langle\langle f\rangle\rangle = \lim_{n\to 0}\frac{[Z^n]-1}{nN} = -\frac{1}{2n}\sum_{\alpha<\beta}(y^{\alpha\beta})^2 - \frac{1}{2n}\sum_\alpha(x^\alpha)^2 - \frac{1}{2n}\sum_\alpha(z^\alpha)^2 + \frac{1}{Nn}\ln\mathrm{Tr}_S e^L + \frac{(1-b^2)^2\beta^2\Delta^2}{4}, \tag{24}$$

$$L = \sum_\theta\left(\Delta'\sum_{\alpha<\beta}(S_\theta^\alpha - b)(S_\theta^\beta - B)y^{\alpha\beta} + \sqrt{K_0}\sum_\alpha(S_\theta^\alpha - b)x^\alpha + \sqrt{K_1}\cos(\theta-\phi)\sum_\alpha(S_\theta^\alpha - b)z^\alpha + [\beta h - \Delta'(1-b^2)]\sum_\alpha(S_\theta^\alpha - b)\right). \tag{25}$$

From the saddle-point condition, the first-order derivative of free energy is zero ($\frac{\partial[f]}{\partial x^\alpha} = \frac{\partial[f]}{\partial y^{\alpha\beta}} = \frac{\partial[f]}{\partial z^\alpha} = 0$), therefore we can obtain the expansion of $\langle\langle f\rangle\rangle$ around the RS point in the following way. We defined $\langle\cdots\rangle_{L_0} = \int\frac{d\theta}{2\pi}\int Dz\exp(L_0)$, and L_0 corresponds to the L replica-symmetry (RS) case. Using $x^\alpha = x + \epsilon^\alpha$, $y^{\alpha\beta} = y + \eta^{\alpha\beta}$, and $z^\alpha = z + \zeta^\alpha$, the expansion of $\beta\langle\langle f\rangle\rangle$ around the RS solution up to second order is

$$\beta\langle\langle f\rangle\rangle = \beta\langle\langle f\rangle\rangle_{L_0} + \frac{1}{2}\Bigg(\sum_{\alpha,\beta}\frac{\partial^2 f}{\partial x^\alpha \partial x^\beta}\epsilon^\alpha\epsilon^\beta + \sum_{\alpha<\beta}\sum_{\gamma<\delta}\frac{\partial^2 f}{\partial y^{\alpha\beta}\partial y^{\gamma\delta}}\eta^{\alpha\beta}\eta^{\gamma\delta} + \sum_{\alpha,\beta}\frac{\partial^2 f}{\partial z^\alpha \partial z^\beta}\zeta^\alpha\zeta^\beta + \sum_{\alpha}\sum_{\beta<\gamma}\frac{\partial^2 f}{\partial x^\alpha \partial y^{\beta\gamma}}\epsilon^\alpha\eta^{\beta\gamma}$$
$$+ \sum_{\alpha<\beta}\sum_{\gamma}\frac{\partial^2 f}{\partial y^{\alpha\beta}\partial z^\gamma}\eta^{\alpha\beta}\zeta^\gamma + \sum_{\alpha,\beta}\frac{\partial^2 f}{\partial x^\alpha \partial z^\beta}\epsilon^\alpha\zeta^\beta\Bigg) \tag{26}$$

$$= \beta\langle\langle f\rangle\rangle_{L_0} + \frac{1}{2}\Bigg(\sum_{\alpha,\beta}G_{\alpha\beta}\epsilon^\alpha\epsilon^\beta + \sum_{\alpha<\beta}\sum_{\gamma<\delta}G_{(\alpha\beta)(\gamma\delta)}\eta^{\alpha\beta}\eta^{\gamma\delta} + \sum_{\alpha,\beta}G^{\alpha\beta}\zeta^\alpha\zeta^\beta + \sum_{\alpha}\sum_{\beta<\gamma}G_{\alpha(\beta\gamma)}\epsilon^\alpha\eta^{\beta\gamma}$$
$$+ \sum_{\alpha<\beta}\sum_{\gamma}G^\gamma_{(\alpha\beta)}\eta^{\alpha\beta}\zeta^\gamma + \sum_{\alpha,\beta}G^\beta_\alpha\epsilon^\alpha\zeta^\beta\Bigg), \tag{27}$$

where G is the Hessian matrix. We have defined the superscripts and subscripts of G as follows; single Hessian subscripts, G_α, indicate the derivative of $\langle\langle f\rangle\rangle$ with respect to the ferromagnetic deviation x. Similarly, a couple of subscripts with braces, $G_{(\alpha\beta)}$, are with respect to y, and single superscripts of Hessian, G^α, are with respect to z. The combination of the replica gives 13 G values. Since the expression of each term of the Hessian is complicated, we further introduce the following definitions to simplify the expression of the Hessian:

$$t_0 = \int\frac{d\theta}{2\pi}\int Dz(\tanh\beta\Psi_\theta - b)^3, \tag{28}$$

$$r_0 = \int\frac{d\theta}{2\pi}\int Dz(\tanh\beta\Psi_\theta - b)^4, \tag{29}$$

$$q_1 = \int\frac{d\theta}{2\pi}\int Dz(\tanh\beta\Psi_\theta - b)^2\cos(\theta-\phi), \tag{30}$$

$$t_1 = \int\frac{d\theta}{2\pi}\int Dz(\tanh\beta\Psi_\theta - b)^3\cos(\theta-\phi), \tag{31}$$

$$m_2 = \int\frac{d\theta}{2\pi}\int Dz(\tanh\beta\Psi_\theta - b)\cos(2\theta-\phi), \tag{32}$$

$$q_2 = \int\frac{d\theta}{2\pi}\int Dz(\tanh\beta\Psi_\theta - b)^2\cos(2\theta-\phi). \tag{33}$$

The coefficients of ϵ that have the form of a RS solution are

$$G_{\alpha\alpha} = 1 - K_0(1 - b^2 - 2bm_0 - m_0^2) \equiv A, \tag{34}$$

$$G_{\alpha\beta} = -K_0(q_0 - m_0^2) \equiv B. \tag{35}$$

The coefficients of ϵ and η cross terms have the form

$$G_{(\alpha\beta)\alpha} = \Delta'\sqrt{K_0}[-(1-b^2)m_0 - 2bq_0 - m_0q_0] \equiv C, \tag{36}$$

$$G_{(\alpha\beta)\gamma} = \Delta'\sqrt{K_0}(-t_0 - m_0q_0) \equiv D. \tag{37}$$

The coefficients of η have the form

$$G_{(\alpha\beta)(\alpha\beta)} = 1 - (\Delta')^2[(1-b^2)^2 - 4b(1-b^2)m_0 + 4b^2q_0 - q_0^2] \equiv P, \tag{38}$$

$$G_{(\alpha\beta)(\alpha\gamma)} = -(\Delta')^2[(1-b^2)q_0 - 2bt_0 - q_0^2] \equiv Q, \tag{39}$$

$$G_{(\alpha\beta)(\gamma\delta)} = -(\Delta')^2(r_0 - q_0^2) \equiv R. \tag{40}$$

The coefficients of η and ζ cross term have the form

$$G^\alpha_{(\alpha\beta)} = \Delta'\sqrt{K_1}[-(1-b^2)m_1 - 2bq_1 - m_1q_0] \equiv C', \tag{41}$$

$$G^\gamma_{(\alpha\beta)} = \Delta'\sqrt{K_1}(t_1 - m_1q_0) \equiv D'. \tag{42}$$

The coefficients of ζ have the form

$$G^{\alpha\alpha} = 1 - K_1\left(\frac{1-b^2}{2} - bm_0 - bm_2 - (m_1)^2\right) \equiv A', \tag{43}$$

$$G^{\alpha\beta} = -K_1\left(\frac{q_0}{2} + \frac{q_2}{2} - (m_1)^2\right) \equiv B'. \tag{44}$$

Finally, the coefficients of ϵ and ζ cross term have the form

$$G^\alpha_\alpha = -\sqrt{K_0K_1}(-2bm_1 - m_0m_1) \equiv E, \tag{45}$$

$$G^\alpha_\beta = -\sqrt{K_0K_1}(q_1 - m_0m_1) \equiv F. \tag{46}$$

A. RSB conditions of SK-type network ($J_1=0$)

First, we take into consideration a network model without spatially organized connectivity ($J_1=0$). The first eigenvalue we take into account is the longitudinal mode where the perturbations are symmetric to the interchange of the replicas. The eigenvalue λ_1 in the longitudinal mode satisfies

$$\begin{bmatrix} A-B & -(C-D) \\ 2(C-D) & P-4Q+3R \end{bmatrix} x = \lambda_1 x. \tag{47}$$

Therefore, the eigenvalue λ_1 is given as

$$\lambda_1 = \{(A-B) + (P-4Q + 3R) \pm \sqrt{[(A-B)-(P-4Q+3R)]^2 + 8(C-D)^2}\}/2. \quad (48)$$

In the limit of $n \to 0$, $A-B$, and $P-4Q+3R$ represent the following:

$$A - B = \frac{1}{J_0 + 2b^2\beta\Delta^2}\frac{\partial^2 f}{\partial m^2}, \quad P - 4Q + 3R = -\frac{2}{\beta\Delta^2}\frac{\partial^2 f}{\partial q^2}. \quad (49)$$

Therefore, a necessary condition of RS stability in longitudinal direction is

$$\frac{\partial^2 f}{\partial m^2} > 0 \quad \text{and} \quad \frac{\partial^2 f}{\partial q^2} < 0. \quad (50)$$

When the above necessary condition is satisfied, the eigenvalue of a longitudinal mode is always positive and RSB in the longitudinal mode does not occur. However, this argument is not always true because $\frac{\partial^2 f}{\partial m^2}$ can be negative as we will show later. One way to check the stability of a RS solution in the longitudinal direction is to calculate Eq. (48) numerically. However, we can show that RS solutions are always stable to the perturbation in longitudinal direction if we numerically solve the saddle-point equations correctly. The details are shown in the Appendix. The other type of perturbation is symmetric under the interchanges of all the replicas but one. This eigenvalue is equivalent to λ_1 for $n=0$.

We then look for an eigenvector that has $\eta^{\zeta\xi}=c$ for specific replicas ζ, ξ, and $\eta^{\zeta\alpha}=\eta^{\xi\alpha}=d$, for any α, and $\eta^{\alpha\beta}=e$ for the other replicas. This mode is called the replicon mode, and the eigenvalue λ_3 for the replicon mode at $n \to 0$ limit is

$$\lambda_3 = P - 2Q + R. \quad (51)$$

From Eq. (51), the replica-symmetry breaking (RSB) condition in the replicon mode is

$$\frac{1}{\beta^2\Delta^2} = \int_{-\pi}^{\pi}\frac{d\theta}{2\pi}\int Dz\, \mathrm{sech}^4[\beta H(z,\theta)]. \quad (52)$$

B. Mexican-hat-type network ($J_1 > 0$)

When we introduce the Mexican-hat-type interaction J_1, the eigenvalue of the longitudinal mode becomes complicated, and here we just show the result. The eigenvalue λ_1 of the longitudinal mode is given by the solution of the following equation:

$$\lambda_1^3 - S\lambda_1^2 + T\lambda_1 + U = 0, \quad (53)$$

where

$$S = (A-B) + (A'-B') + (P-4Q+3R), \quad (54)$$

$$T = (A-B)(A'-B') + (A'-B')(P-4Q+3R) + (P-4Q+3R)(A-B) - (E-F)^2 + 2(C'-D')^2 + 2(C-D)^2, \quad (55)$$

$$U = 2(A-B)(C'-D')^2 + 2(A'-B')(C-D)^2 + (P-4Q+3R)(E-F)^2 - (A-B)(A'-B')(P-4Q+3R) + 4(C-D)(E-F)(C'-D'). \quad (56)$$

Again, a way to check the stability in the longitudinal mode is to directly solve Eq. (53), but we can show that λ_1 is always positive in a certain condition, as shown in the Appendix. The condition where the eigenvalue of the replicon mode becomes zero (RSB condition) is equivalent to Eq. (52).

V. RESULTS

A. No spatial modulation case ($J_1=0$)

First, we compare the Ising spin and McCulloch-Pitts neuron models without spatially modulated interaction ($J_1=0$). As the parameter b changes, the external field also effectively changes [Eq. (6)]. To remove this effect, we set $h=-J_0 b$ throughout this paper. In Fig. 2, we show the analytical calculation of m_0 obtained from Eqs. (19)–(22) and the simulation results. The simulation results support our theoretical calculation for both the Ising spin model ($b=0$) and McCulloch-Pitts neuron model ($b=-1.0$) at $1/\beta\Delta=0.7$ and $J_0/\Delta=1.5$. The qualitative difference is that the second-order transition for the Ising spin model ($b=0$) is not observed in the McCulloch-Pitts neuron network.

Networks of McCulloch-Pitts neurons have different constraints due to its asymmetric states and the conventional definition of the phases in an Ising spin network cannot be directly adopted. For example, McCulloch-Pitts networks can have a bistable region at low and high m_0 values [Figs. 2(b) and 2(c)]. The ferromagnetic (F) state in an Ising spin network also has bistability at m_0, and therefore we have defined F phase as the bistability in the m_0 value. McCulloch-Pitts networks can also have monostable states in the m_0 value, but q_0 is always positive. The only distinction between the spin-glass (SG) state and the paramagnetic (P) state is whether RSB occurs or not. Thus we define the SG state as monostability in m_0 value with RSB, and the P state as monostability in m_0 value without RSB (RS stable). We will introduce a spatially organized interaction J_1 later in this paper. For large J_1, a network can have a localized (L) state ($m_1 \neq 0$). To summarize, we define the state as follows so that we can use the same definitions for both models: For the ferromagnetic (F) state, bistability in m_0, and $m_1=0$; spin-glass (SG) state, monostability in m_0, $m_1=0$, and RSB occurs; paramagnetic (P) state, monostability in m_0, $m_1=0$, and RS stable; localized (L) state, $m_0 \neq 0$ and $m_1 \neq 0$; In F and L states, there can be a RS stable or a RSB region.

By using the above definition of the states, we draw the phase diagram in Fig. 3 at various control parameters b. First the distinction between an Ising spin network and a McCulloch-Pitts network is the wide range of the $\partial^2 f/\partial m_0^2 < 0$ region for $b \neq 0$ cases [Figs. 3(b) and 3(c)] which is not found in cases where $b=0$. For the better understanding of this phenomena, we show the landscape of free energy at

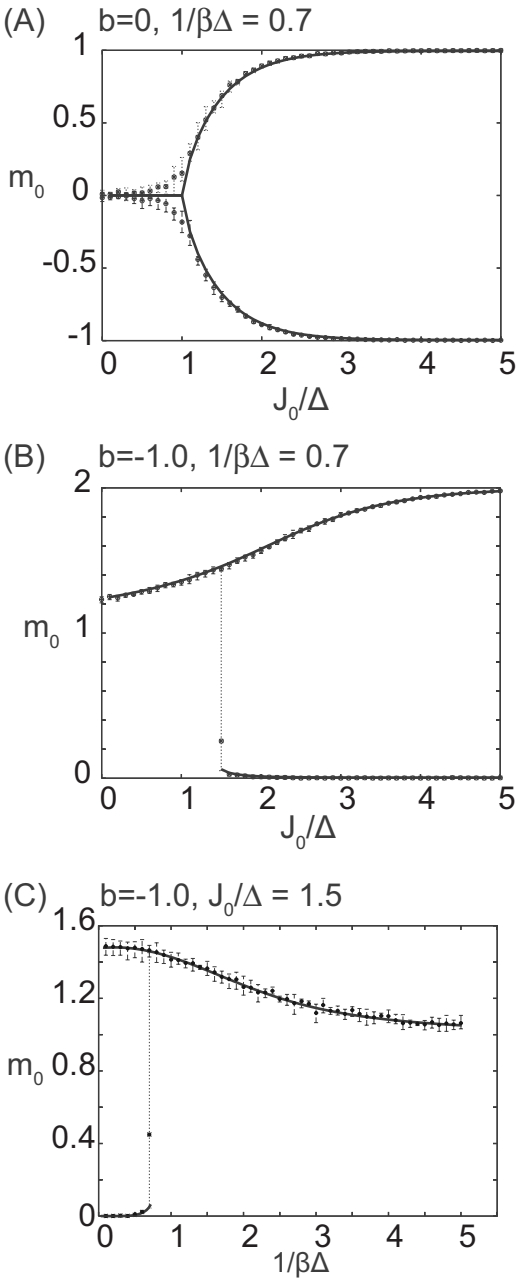

FIG. 2. Typical value of m_0 for various parameters of b, $\beta\Delta$, and J_0/Δ for $J_1=0$ (homogeneous) network. Solid lines are analytical calculations from Eqs. (19)–(22). The error bars were obtained from the 11 samples of simulations. (a) $b=0$, $1/\beta\Delta=0.7$. (b) $b=-1.0$, $1/\beta\Delta=0.7$. (c) $b=-1.0$, $J_0/\Delta=1.5$.

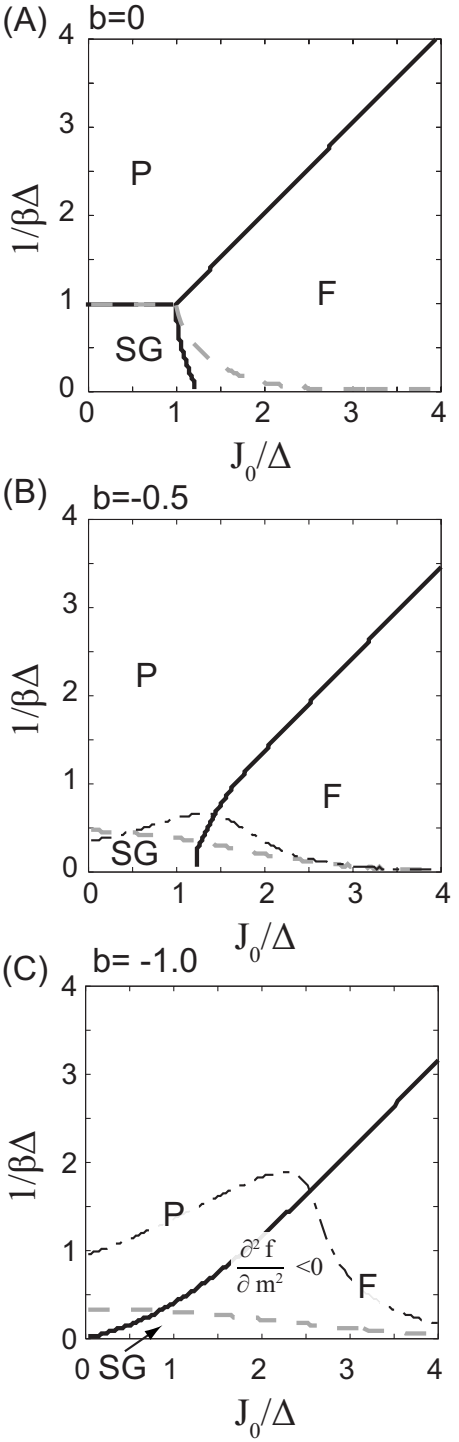

FIG. 3. Phase diagrams of networks without Mexican-hat interaction ($J_1=0$), shown in $J_0/\Delta-1/\beta\Delta$ space for various control parameter b; (a) $b=0$, (b) $b=-0.5$, and (c) $b=-1.0$. The regions under the solid lines are the ferromagnetic phase. The gray broken lines represent the AT lines. The region under thin dashed-dotted lines are with $\frac{\partial^2 f}{\partial m^2}<0$. The region with $\frac{\partial^2 f}{\partial m^2}<0$ expands as b decreases.

$(J_0/\Delta, 1/\beta\Delta)=(1.5, 0.5)$ at various control parameters b in Fig. 4. At the point where $(J_0/\Delta, 1/\beta\Delta)=(1.5, 0.5)$, the network is always in the F phase for the whole range of $-1 \leqslant b \leqslant 0$ and always has bistability. There are three intersections of a maximum q_0 and extremal values of m_0. The outer two are the stable equilibrium states for these three cases. When $b=0$, the outer intersections are made by the maximum line of q_0 and minimum lines of m_0. As b deviates from zero, the intersection is formed by the maximum of q_0 and maximum of m_0 and the second derivative of free energy by m_0, $\partial^2 f/\partial m_0^2$, changes from positive to negative [Fig. 4(c)].

For an Ising spin network, $\partial^2 f/\partial m_0^2>0$ is always satisfied and there is no need to check Eq. (48). However, for the McCulloch-Pitts neuron network, we found that $\partial^2 f/\partial m_0^2 > 0$ is not always satisfied and we must take into account the necessary and sufficient condition in Eq. (48) in addition to

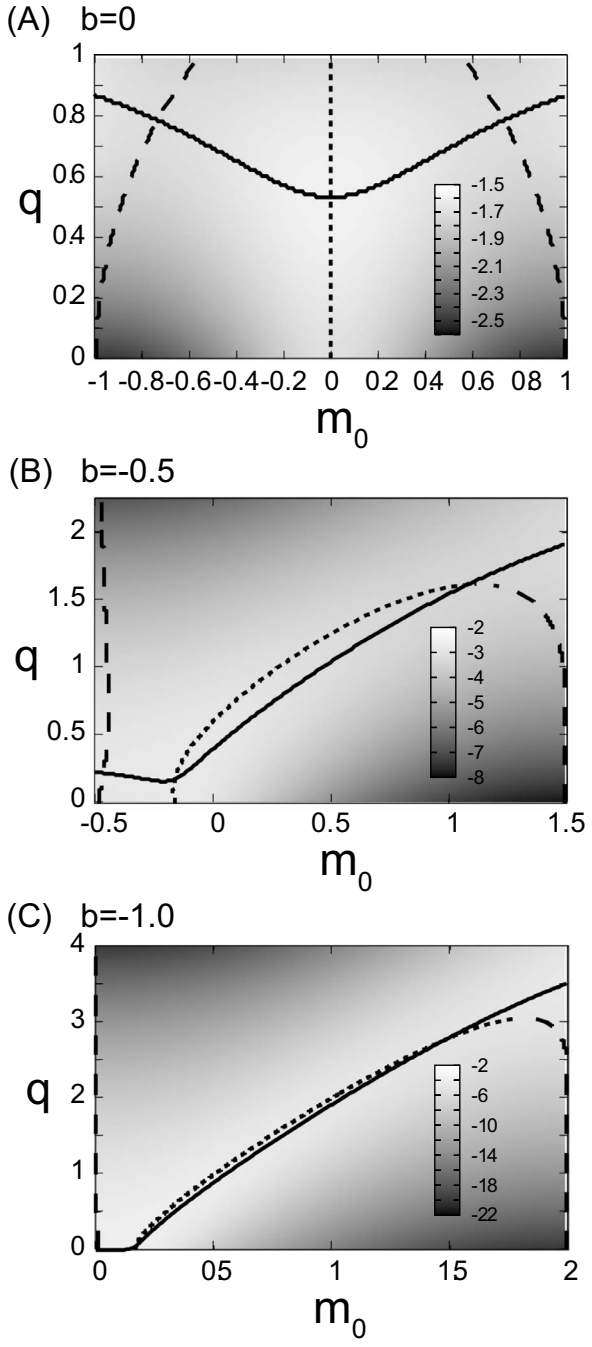

FIG. 4. The free-energy landscapes at $(J_0/\Delta, 1/\beta\Delta)=(1.5, 0.5)$. (a) Ising spin model ($b=0$). (b) $b=-0.5$. (c) McCulloch-Pitts neuron model ($b=-1.0$). The maximum value in the q direction is shown as a solid line. The maximum (minimum) value in the m direction is shown as a dotted (dashed) line.

the standard RSB condition in Eq. (51). We, however, found that we have proof that RS solutions are always stable in the longitudinal direction. Therefore, this apparent distinction of $\frac{\partial^2 f}{\partial m_0^2}$ between the Ising spin and McCulloch-Pitts networks did not result in a qualitative difference, but we reported this issue because conventional arguments often consider the necessary condition of Eq. (50) only, and in general, such arguments cannot justify the stability of the RS solution in the longitudinal direction. Our proof in the Appendix gives general reasoning as to why we do not need to take into account the RSB in the longitudinal direction.

B. Networks with Mexican-hat interaction and quenched randomness ($J_1 \neq 0$)

In this section, we take into consideration a network with spatially modulated interaction ($J_1 \neq 0$) with quenched noise. Now there are three order parameters, and the phase diagram is three dimensional. For simplicity, we fixed $1/\beta\Delta=0.3$ and study the phase diagram in this section.

In Fig. 5, we show the analytical calculation of the order parameters m_0 and m_1 in the Ising spin network ($b=0$) at $J_1/\Delta=5.5$. To clarify the hysteresis in this system, let us start by introducing the following two cases: Increasing J_0/Δ [Fig. 5(a)] and decreasing J_0/Δ [Fig. 5(b)]. When the uniform interaction term J_0 is relatively small, the L phase is stable. The phase transition point depends on the history as shown in Figs. 5(a) and 5(b). Figure 5(c) is a summary of these results to show the bistable region shown as L+F.

Next, we show the phase diagram in the Mexican-hat-type network composed of Ising spins ($b=0$). The RSB regions calculated from Eq. (52) are shown in the shaded region in Fig. 6. In the dark shaded region, the RSB occurs only in the L phase.

Finally, we studied the McCulloch-Pitts neuron networks. Figure 7 shows the analytical calculation of the order parameters m_0 and m_1 at $J_1/\Delta=5.5$. This network also shows hysteresis, and to clarify the difference in phase transition points, we again show the analytical calculations by gradually increasing and decreasing J_0/Δ in Figs. 7(a) and 7(b). When the network starts from a localized state (L phase) and J_0/Δ is gradually increased from zero, the phase transition from the L to F phase occurs around $J_0/\Delta \approx 2.1$. On the other hand, when the network starts from a high J_0/Δ parameter, the network has two stable, uniformly active states; high m_0 and low m_0. The high m_0 state is regarded as an active state for the neural network, and the low m_0 state represents the spontaneous, relatively low activity states. As J_0/Δ gradually decreases, the high m_0 state shows a phase transition in the L phase around $J_0/\Delta \approx 1.6$ which is slightly lower than the transition from L to F. If the initial state of the network is the low m_0 state in F phase, it is stable until $J_0/\Delta \approx 0.8$ and finally makes a transition to the L phase. To summarize, there are four network states as shown in Fig. 7(c). A schematic picture of the stable states is also shown above the figure; L for the phase where localized activity state is the only stable state. L+P represents the phase where the localized state and paramagnetic state coexist. L+F is the phase where the localized state and the ferromagnetic (bistable m_0) state coexist. The F phase is the phase where the ferromagnetic state is stable. We noted that depending on the parameters, it is possible that F phase makes a transition again to the P state for very large J_0/Δ values (data not shown).

The phase diagram of a McCulloch-Pitts neuron network is shown in Fig. 8. The phase transitions are shown with the solid lines, and Almeida-Thouless (AT) lines are shown with dashed lines. As the localized interaction J_1/Δ increases, the L phase becomes stable. As the uniform interaction J_0/Δ

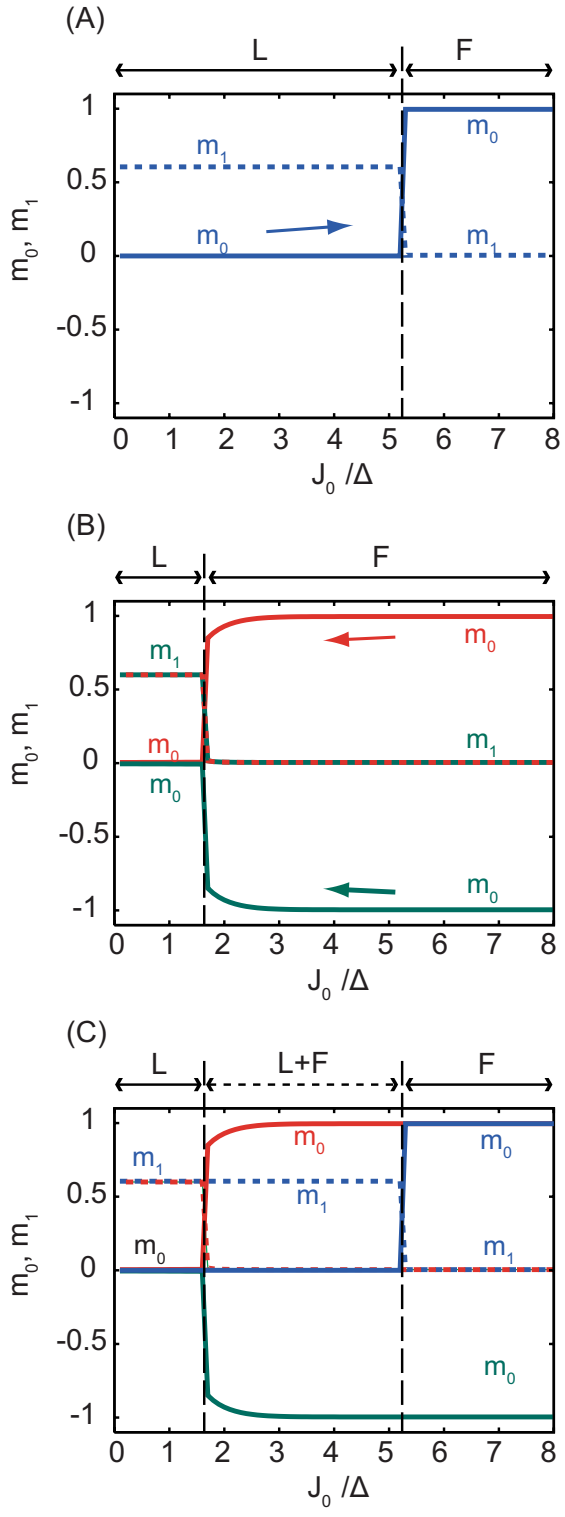

FIG. 5. (Color online) Analytical calculation of order parameters at $b=0, J_1/\Delta=5.5$ intersection. Solid lines represent m_0, and the dotted lines represent m_1. The hysteresis reveals the bistable phase in the midrange of J_0/Δ. (a) Localized phase is stable until $J_0/\Delta \sim 5.3$ and makes a phase transition to the ferromagnetic phase when J_0/Δ is gradually increased. (b) Ferromagnetic phase is stable until $J_0/\Delta \sim 1.6$ and makes a phase transition to the local phase when J_0/Δ is gradually decreased. (c) Overlay of (a) and (b). There is a bistable phase around $1.6 < J_0/\Delta < 5.3$ for this parameter set.

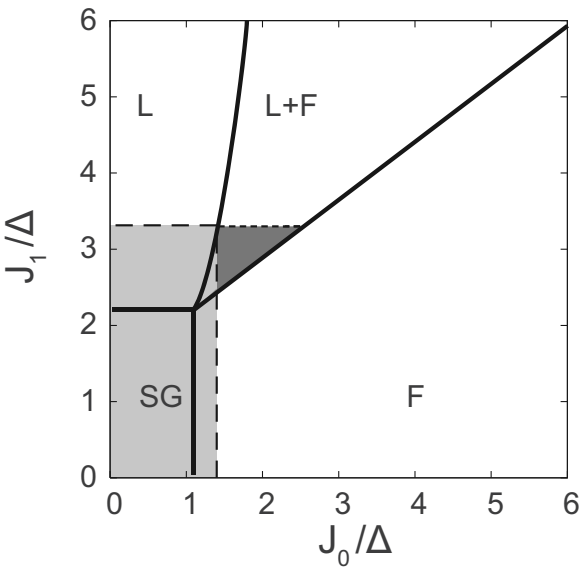

FIG. 6. Phase diagram of Ising spin network ($b=0$) at $1/\beta\Delta=0.3$. The RSB region calculated from eq. (52) is shown in the light-shaded region. Only the RSB region in the local phase is shown in the dark-shaded region.

increases, the F phase becomes stable. In between them, there are two type of bistable or tristable phases. For the lower J_0/Δ region, one finds the phase where the L state and P state are stable (L+P). For the higher J_0/Δ region, there is a phase with the L state and F state (L+F). In this L+F phase, there are three stable states; low m_0 and high m_0 with $m_1=0$, and $m_0, m_1 \neq 0$. The AT line calculated from Eq. (52) is shown in the shaded regions. In the dark shaded region in the F phase, the RSB occurs only in the high m_0 state.

VI. CONCLUSION AND DISCUSSION

In this paper, the stability of replica-symmetry ansatz in the Ising spin and McCulloch-Pitts neuron networks were compared. While studying the necessary and sufficient conditions of the RSB, we found that a necessary condition to ensure stability of the RS solution in the longitudinal mode, which is often used in the literature [1], is not satisfied in asymmetric state systems. We studied the RSB condition in the longitudinal mode and found that it will not occur neither in the symmetric nor asymmetric state system. The proof on this is outlined in the Appendix.

The effect of asymmetry of the binary state on the AT line is not straightforward. For lower J_0/Δ values, RS solutions are more stable for a relative noise level of $1/\beta\Delta$. On the other hand, for larger J_0/Δ values, the RS solutions are less stable for the same value of $1/\beta\Delta$.

In this paper, we have not considered the plasticity, or the mechanism of generating symmetric noisy interaction in our model. There have been several models of the formation of stable orientation tunings and spatial working memory [18,22]. Further analysis of such models and the experimental clarification of the neural substrates of learning would be required for the better understanding of the stable information representation in the cortex.

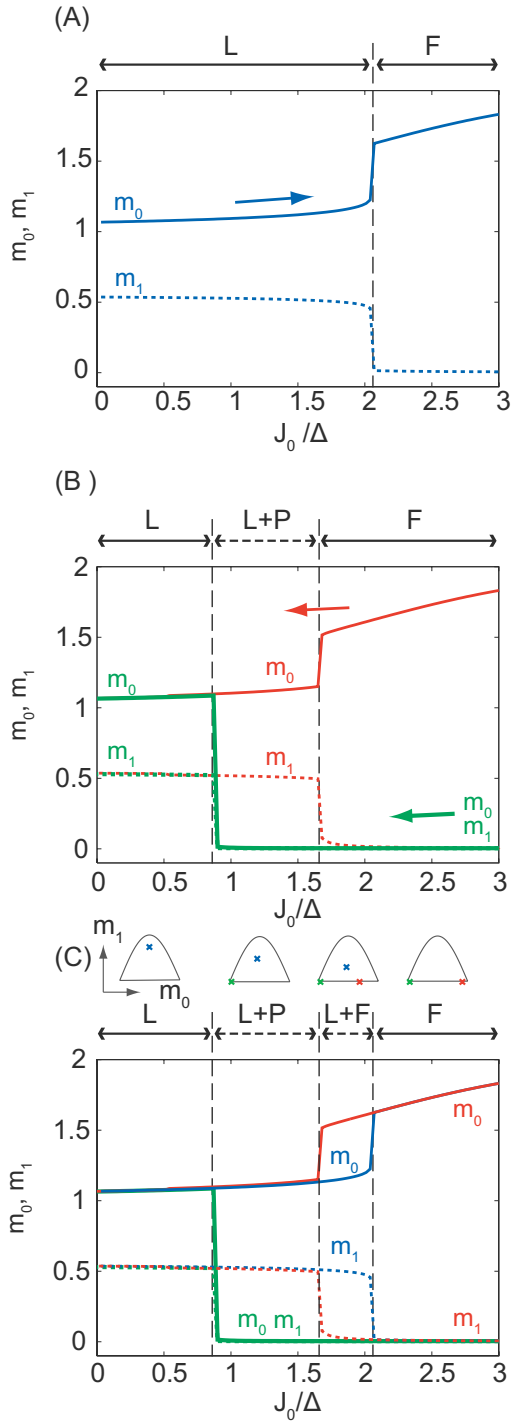

FIG. 7. (Color online) Analytical calculation of order parameters at $b=-1.0$, $J_1/\Delta=5.5$ intersection. The solid lines represent m_0, and dotted lines represent m_1. The hysteresis reveals the bistable phase in the midrange of J_0/Δ. (a) Local phase is stable until $J_0/\Delta \sim 2.1$ as J_0/Δ is gradually increased, then the ferromagnetic phase becomes dominant. (b) Initially, the ferromagnetic phase has bistability at low and high m_0 values. When J_0/Δ is gradually decreased, this bistability loses its stability at $J_0/\Delta \sim 1.6$. (c) Overlay of (a) and (b). There is a bistable region with one local and one uniformly active states around $0.8 < J_0/\Delta < 1.6$, and a tristable region with one local and two uniformly active states around $1.6 < J_0/\Delta < 2.1$ for this parameter set. The schematic positions of the stable states in the m_0-m_1 space are also shown above.

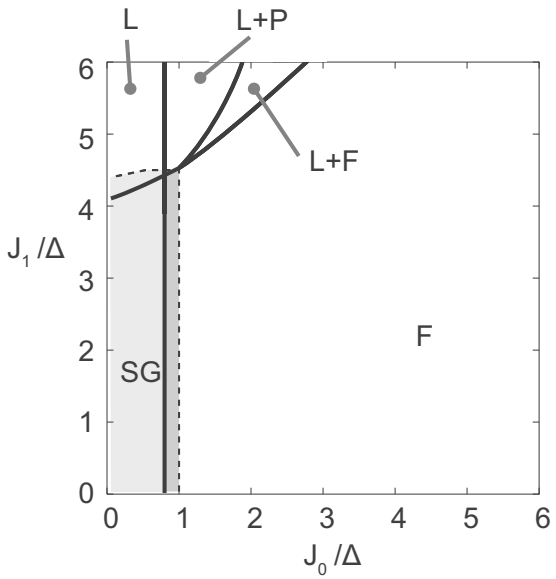

FIG. 8. Phase diagram of McCulloch-Pitts network ($b=-1.0$) at $1/\beta\Delta=0.3$. The RSB regions are illustrated in the same way as shown in Fig. 6.

ACKNOWLEDGMENTS

This work was partially supported by a Grant-in-Aid for Scientific Research on Priority Areas Grant No. 18079003 from the Ministry of Education, Culture, Sports, Science and Technology of Japan. K.H. is supported by JSPS.

APPENDIX: STABILITY OF LONGITUDINAL MODE IS EQUAL TO THE STABILITY OF PSEUDODYNAMICS

In this appendix, we show that longitudinal RSB will not occur. This is because the RSB condition in the longitudinal mode is equivalent to the stability condition of the pseudodynamics we use to search for the stable state. For simplicity, we focus on $J_1=0$, but it can be extended to any value of J_1 using the similar arguments.

First, we solve the saddle-point equations of the following free energy:

$$-\beta[f] = -\frac{\beta J_0 + 2b^2\beta^2\Delta^2}{2}m_0^2 + \frac{\beta^2\Delta^2}{4}(1-b-q_0)^2 + \int_{-\infty}^{\infty} Dz \ln\{\exp[(1-b)\Psi_\theta] + \exp[(-1-b)\Psi_\theta]\}. \tag{A1}$$

It corresponds to the SK model when $b=0$, and the McCulloch-Pitts model when $b=-1$. The saddle-node condition is

$$\frac{\partial f}{\partial m_0} = 0 = K_0 m_0 - K_0 \int Dz(\tanh\Psi - b), \tag{A2}$$

$$\frac{\partial f}{\partial q} = 0 = -\frac{\Delta'^2}{2}q + \frac{\Delta'^2}{2}\int Dz(\tanh \Psi - b)^2, \qquad \text{(A3)}$$

where $\Delta' = \beta\Delta$, $K_0 = (\beta J_0 + 2b^2\beta^2\Delta^2)$. We solve this nonlinear equations by using a gradient-descent method or pseudodynamics as follows:

$$\dot{m}_0 = -\frac{1}{K_0}\frac{\partial f}{\partial m_0} = -m_0 + \int Dz(\tanh \Psi - b), \qquad \text{(A4)}$$

$$\dot{q} = \frac{2}{\Delta'^2}\frac{\partial f}{\partial q} = -q + \int Dz(\tanh \Psi - b)^2. \qquad \text{(A5)}$$

Note that the solution is searched for in the direction of the gradient descent in the m_0 direction, and for the gradient ascent in the q direction. This gives us the saddle-node points of the free energy f. Now, let us note that a dynamical system

$$\boldsymbol{x} = F(\dot{\boldsymbol{x}}) \qquad \text{(A6)}$$

has a stable equilibrium point $\boldsymbol{x}^*$, if $F(\boldsymbol{x}^*)=0$ and all the eigenvalues of the Jacobian matrix J have negative real part. For a two-dimensional system, the Jacobian matrix is

$$J = \begin{bmatrix} \frac{\partial F_1}{\partial x_1} & \frac{\partial F_1}{\partial x_2} \\ \frac{\partial F_2}{\partial x_1} & \frac{\partial F_2}{\partial x_2} \end{bmatrix}. \qquad \text{(A7)}$$

Therefore, in our case, the Jacobian matrix J evaluated at a stable solution (m_0^*, q^*) is

$$J = \begin{bmatrix} -\frac{1}{K_0}\frac{\partial^2 f}{\partial m_0^2} & -\frac{1}{K_0}\frac{\partial^2 f}{\partial m_0 \partial q} \\ \frac{2}{\Delta'^2}\frac{\partial^2 f}{\partial m_0 \partial q} & \frac{2}{\Delta'^2}\frac{\partial^2 f}{\partial q^2} \end{bmatrix} = K^2\ddot{F},$$

where

$$K = \begin{bmatrix} 1/\sqrt{K_0} & 0 \\ 0 & \sqrt{2}/\Delta' \end{bmatrix}, \quad \ddot{F} = \begin{bmatrix} -\frac{\partial^2 f}{\partial m_0^2} & -\frac{\partial^2 f}{\partial m_0 \partial q} \\ \frac{\partial^2 f}{\partial m_0 \partial q} & \frac{\partial^2 f}{\partial q^2} \end{bmatrix}. \qquad \text{(A8)}$$

The Jacobian matrix J must have negative eigenvalues if our solution is stable for the dynamics of Eqs. (A4) and (A5). In practice, since we solve the dynamics forward in time, our solution provides a Jacobian with negative eigenvalues.

Next, let us compare the condition of stability of the RS solution in the longitudinal mode and matrix J. The RS stable condition is that the following eigenvalue λ has positive real part:

$$H\mu = \begin{bmatrix} A-B & -(C-D) \\ 2(C-D) & P-4Q+3R \end{bmatrix}\mu = \lambda\mu. \qquad \text{(A9)}$$

By using the relations $A-B = K_0^{-1}\frac{\partial^2 f}{\partial m_0^2}$, $C-D = -1/(\Delta'\sqrt{K_0})\frac{\partial^2 f}{\partial m_0 \partial q}$, and $P-4Q+3R = -2/\Delta'^2\frac{\partial^2 f}{\partial q^2}$, we found that

$$H = \begin{bmatrix} K_0^{-1}\frac{\partial^2 f}{\partial m_0^2} & 1/(\Delta'\sqrt{K_0})\frac{\partial^2 f}{\partial m_0 \partial q} \\ -2/(\Delta'\sqrt{K_0})\frac{\partial^2 f}{\partial m_0 \partial q} & -2/\Delta'^2\frac{\partial^2 f}{\partial q^2} \end{bmatrix} = -K^{\top}\ddot{F}K. \qquad \text{(A10)}$$

The relationship between J and H is

$$-K^{-1}JK = -K^{\top}\ddot{F}K = H. \qquad \text{(A11)}$$

Here we have used the relation $K^{\top} = K$. Therefore, the relationship between J and H is the similar matrix with a changing sign. The similar matrices have the same eigenvalues, and the coefficient of -1 changes the sign of the eigenvalues. This means that, if a Jacobian matrix J has negative eigenvalues (stable solution of pseudodynamics), the Hessian matrix H should have positive eigenvalues (local minimum of free energy in the direction of the longitudinal mode).

To summarize, the stable solutions calculated by the pseudodynamics in Eqs. (A4) and (A5) are always stable in the longitudinal mode direction. Therefore, there is no longitudinal RSB.

[1] Hidetoshi Nishimori, *Statistical Physics of Spin Glasses and Information Processing: An Introduction* (Oxford University Press, Oxford 2001).

[2] Daniel J. Amit, Hanoch Gutfreund, and H. Sompolinsky, Phys. Rev. A **32**, 1007 (1985).

[3] Daniel J. Amit, Hanoch Gutfreund, and H. Sompolinsky, Phys. Rev. Lett. **55**, 1530 (1985).

[4] M. Okada, Neural Networks **8**, 833 (1995).

[5] C. J. Perez Vicente and D. J. Amit, J. Phys. A **22**, 559 (1989).

[6] M. V. Tsodyks and M. V. Feigel'man, Europhys. Lett. **6**, 101 (1988).

[7] M. Okada, Neural Networks **9**, 1429 (1996).

[8] D. J. Amit, H. Gutfreund, and H. Sompolinsky, Phys. Rev. A **35**, 2293 (1987).

[9] D. H. Hubel and T. N. Wiesel, J. Physiol. (London) **160**, 106 (1962).

[10] D. H. Hubel and T. N. Wiesel, Proc. R. Soc. London, Ser. B **198**, 1 (1977).

[11] C. Blakemore, R. H. Carpente, and M. A. Georgeso, Nature (London) **228**, 37 (1970).
[12] H. R. Wilson and J. D. Cowan, Biophys. J. **12**, 1 (1972).
[13] S. Amari, Biol. Cybern. **27**, 77 (1977).
[14] R. Ben-Yishai, R. L. Bar-Or, and H. Sompolinsky, Proc. Natl. Acad. Sci. U.S.A. **92**, 3844 (1995).
[15] A. Roxin, N. Brunel, and D. Hansel, Phys. Rev. Lett. **94**, 238103 (2005).
[16] C. R. Laing and C. C. Chow, Neural Comput. **13**, 1473 (2001).
[17] O. Shriki, D. Hansel, and H. Sompolinsky, Neural Comput. **15**, 1809 (2003).
[18] A. Renart, P. Song, and Xiao-Jing Wang, Neuron **38**, 473 (2003).
[19] K. Hamaguchi, J. P. L. Hatchett, and M. Okada, Phys. Rev. E **73**, 051104 (2006).
[20] S. Funahashi, C. J. Bruce, and P. S. Goldman-Rakic, J. Neurophysiol. **61**, 331 (1989).
[21] J. R. L. de Almeida and D. J. Thouless, J. Phys. A **11**, 983 (1978).
[22] J. A. F. Heimel and H. Sompolinsky, Neurocomputing **38-40**, 1261 (2001).